Available online at www.sciencedirect.com

ScienceDirect

Virology 371 (2008) 108–120

VIROLOGY

www.elsevier.com/locate/yviro

Recruitment of Alix/AIP1 to the plasma membrane by Sendai virus C protein facilitates budding of virus-like particles

Takashi Irie *, Natsuko Nagata, Tetsuya Yoshida, Takemasa Sakaguchi

Department of Virology, Graduate School of Biomedical Sciences, Hiroshima University, 1-2-3 Kasumi, Minami-ku, Hiroshima 734-8551, Japan

Received 20 June 2007; returned to author for revision 2 August 2007; accepted 14 September 2007
Available online 29 October 2007

Abstract

Sendai virus (SeV) is unique in that one of the viral accessory proteins, C, enhances budding of virus-like particles (VLPs) formed by SeV matrix protein M by physically interacting with Alix/AIP1. C protein itself does not have the ability to form VLPs, while M protein provides viral budding force, like other enveloped viruses. Here we show that SeV C protein recruits Alix/AIP1 to the plasma membrane (PM) to facilitate VLP budding. SeV M-VLP budding is sensitive to overexpression of a dominant-negative (DN) form of VPS4A only in the presence of the C proteins, which is able to recruit Alix/AIP1 to the PM. Our results indicate that SeV M and C proteins play separate roles in the budding process: M protein drives budding and C protein enhances the efficiency of the utilization of cellular MVB sorting machinery for efficient VLP budding.

Keywords: Paramyxovirus; Sendai virus; Virus-like particles; Budding; C protein; Alix/AIP1; MVB sorting

Introduction

Since enveloped viruses bud from cellular membranes to acquire lipid-containing envelopes, membrane fission event is essential for them to be efficiently released from host cells at the final step of their lifecycle. Viral matrix and retroviral Gag proteins have been shown to be able to bud from the cell surface by themselves in the form of lipid-enveloped, virus-like particles (VLPs), suggesting that these proteins play important roles in the late-budding step (Bieniasz, 2006). For many enveloped viruses, it has been shown that host cell endosomal sorting machinery is utilized for efficient virus budding (Bieniasz, 2006). This is achieved through an interaction between late-budding (L) domains identified within the viral matrix and Gag proteins and a component of host cellular protein trafficking machinery (Bieniasz, 2006). The major L-domain motifs, PPxY, PT/SAP, YPxL, and/or LxxL have been identified, and have been especially well characterized in retroviruses (Demirov and Freed, 2004; Fisher et al., 2007; Strack et al., 2003). The PPxY-, PT/SAP-, and YPxL/LxxL-types of L-domains have been shown to interact with Nedd4-like E3 ubiquitin ligases, tumor susceptible gene 101 (Tsg101), a member of ESCRT-I (endosomal sorting complex required for transport I), and Alix/AIP1, which has been reported to be linked to ESCRT-I and -III complexes (Demirov and Freed, 2004).

ESCRT complexes play a critical role in sorting proteins into the multivesicular body (MVB) in mammalian cells (Slagsvold et al., 2006). In this process, three ESCRT complexes, ESCRT-I, -II, and -III act in a sequential manner (Babst et al., 2002a,b). In the final step of protein sorting, an AAA-type ATPase VPS4 interacts with ESCRT-III to catalyze the disassembly of ESCRT machinery to recycle its components (Babst et al., 1997, 1998). Since the expression of dominant-negative (DN) forms of VPS4 lacking the ability to bind or hydrolyze ATP was shown, in many cases, to inhibit the budding of VLPs and/or viruses containing any of the major three types of L-domains, it is believed that most viruses possessing these L-domain motifs generally utilize MVB sorting machinery for efficient budding (Bieniasz, 2006). However, for many other enveloped viruses, L-domain motifs have not yet been identified, and whether MVB sorting machinery is involved in the virus budding is still unknown. Recently, in addition to the major L-domain motifs, FPIV, YEIL, and YMYL motifs have been identified as potential L-domains

* Corresponding author. Fax: +81 82 257 5159.
E-mail address: tirie@hiroshima-u.ac.jp (T. Irie).

0042-6822/$ - see front matter © 2007 Elsevier Inc. All rights reserved.
doi:10.1016/j.virol.2007.09.020

within paramyxovirus SV5 M, prototype foamy virus (PFV) Gag, and Nipah virus M proteins, respectively (Ciancanelli and Basler, 2006; Patton et al., 2005; Schmitt et al., 2005). However, the interacting partners of these motifs have not been identified yet. In addition, it should be noted that SV5 M protein alone does not have the ability to bud as VLPs and requires other viral proteins for efficient budding (Schmitt et al., 2002).

As for SeV, a prototype of the family *Paramyxoviridae*, we recently reported that the YLDL motif within M protein is critical for M-VLP budding and physically and functionally interacts with Alix/AIP1 (Irie et al., 2007). In addition, SeV is unique in that one of the viral accessory proteins, C, also physically interacts with Alix/AIP1 in a different manner from the M-Alix/AIP1-interaction, and enhances M-VLP budding, although C protein does not have the ability to form VLPs (Irie et al., 2007; Sakaguchi et al., 2005).

SeV C protein is translated from the −1 reading frame relative to the P gene frame. P protein is initiated at the AUG codon at position 104, whereas four C proteins, C', C, Y1, and Y2, are produced from the initiation codons at positions 81, 114, 183, and 201, respectively (Lamb and Parks, 2006). C proteins are multifunctional proteins involved in regulation of viral RNA synthesis (Curran et al., 1992; Grogan and Moyer, 2001; Horikami et al., 1997), counteracting the innate immune response of the host cell (Garcin et al., 2001, 1999; Gotoh et al., 2003; Kato et al., 2001; Komatsu et al., 2002; Takeuchi et al., 2001), inhibition of virus-induced apoptosis (Koyama et al., 2003), and the efficiency of VLP/virus budding (Irie et al., 2007; Sakaguchi et al., 2005; Sugahara et al., 2004). Recently, it was reported that the unmodified N-terminal 23 amino acids of SeV C protein function as a PM targeting signal and a membrane anchor based on experiments using artificial recombinant C proteins containing reporter tdTomato fluorescent protein, and that localization of C protein at the PM is important for its ability to induce phosphorylated-Stat1 formation in an IFN-independent manner (Marq et al., 2007).

In this report, we show that localization of C protein at the PM is also important for its ability to enhance M-VLP budding, and we discuss a possible mechanism for this enhancement.

Results

The N-terminal 23 amino acids of SeV C protein are important for its ability to localize to the PM

Recently, it has been reported that the unmodified N-terminal 23 amino acids of SeV C protein functions as a PM targeting signal and a membrane anchor, as shown by studies using artificial recombinant C proteins containing reporter tdTomato fluorescent protein (Marq et al., 2007). To examine this ability of the intact C protein without any influence of smaller C proteins synthesized from the downstream initiation codons, we constructed a series of C protein mutants in which the initiation codons for Y1 and/or Y2 were replaced by ACG, resulting in amino acid changes of methionine to threonine (Fig. 1A). In addition, three C-terminal deletion mutants were constructed in the C-d2Y backbone (Fig. 1A).

At first, the cellular localization of these C mutants was analyzed by immunofluorescence microscopy using anti-C pAb (Fig. 1B). As expected from the recent report by Marq et al. (2007), in the C-WT-transfected cells where smaller amounts of Y1 and Y2 as well as C proteins were produced, fluorescence was predominantly detected at the cell periphery; intracellular membranes and cytosol were hardly fluorescent (Fig. 1B, upper left). Predominant localization of the fluorescence at the PM was also observed in the C-dY1 and C-d2Y-transfected cells lacking Y1 and both Y1 and Y2 protein expression, respectively (Fig. 1B, middle left and right). Interestingly, in addition to the localization at the cell periphery, weaker fluorescence was detected at the nuclear envelope in the C-dY2-transfected cells where C and Y1 proteins were produced (Fig. 1B, middle). In the C-terminal deletion mutant-transfected cells, fluorescence was still mainly observed at the cell periphery, although localization probably at intracellular membranes and granular distribution throughout the cytoplasm appeared in accordance with the length of the C-terminal deletion (Fig. 1B, bottom left, and data not shown). In contrast to these C mutants, diffuse cytoplasmic and nuclear localization was observed in the Y1-transfected cells where Y2 as well as Y1 proteins were produced, but localization at the PM was not detectable (Fig. 1B, upper middle). In some of the Y1-transfected cells, fluorescence was predominantly detected in the nucleus (Fig. 1B, upper right). Similar subcellular localization was observed in the Y1-dY2-transfected cells where only Y1 protein was produced and in the Y2-transfected cells (Fig. 1B, bottom middle and bottom right).

The localization of these C mutants was also examined by subcellular fractionation (Figs. 1C and D). Cytosolic (S) and membrane (P) fractions were prepared from the post-nuclear supernatant (PNS) of C mutant-transfected 293T cells, and the protein expression in equal amounts of each sample was compared by Western blotting using anti-C pAb followed by quantitative analysis using an LAS-1000 luminescent image analyzer. SeV HN-transfected samples served as a control for membrane-targeted proteins. As expected, most of the HN protein was detected in the membrane fraction and almost none in the cytosolic fraction (Figs. 1C, lanes 21 and 22, and D). In accord with the results of Fig. 1B, C-WT as well as all of the C mutants retaining an intact N-terminus were predominantly detected in the membrane fractions, with membrane to cytosolic ratios ranging from approximately 11 to 26 (Figs. 1C, lanes 1–14, and D). In contrast, similar amounts of Y1, Y1-dY2, and Y2 proteins were detected in the cytosolic and membrane fractions (Figs. 1C, lanes 15–20, and D).

These results indicate that the N-terminal 23 amino acid region of SeV C protein was important for its ability to associate with the PM, and that the additional expression of Y1 and/or Y2 proteins from downstream AUG codons of the transfected-C mutants was not required for this ability.

Localization of SeV C protein at the PM is important for its ability to enhance SeV M-VLP budding

Budding of SeV and SeV VLPs occurs at the PM, and we previously reported that SeV C protein could enhance M-VLP

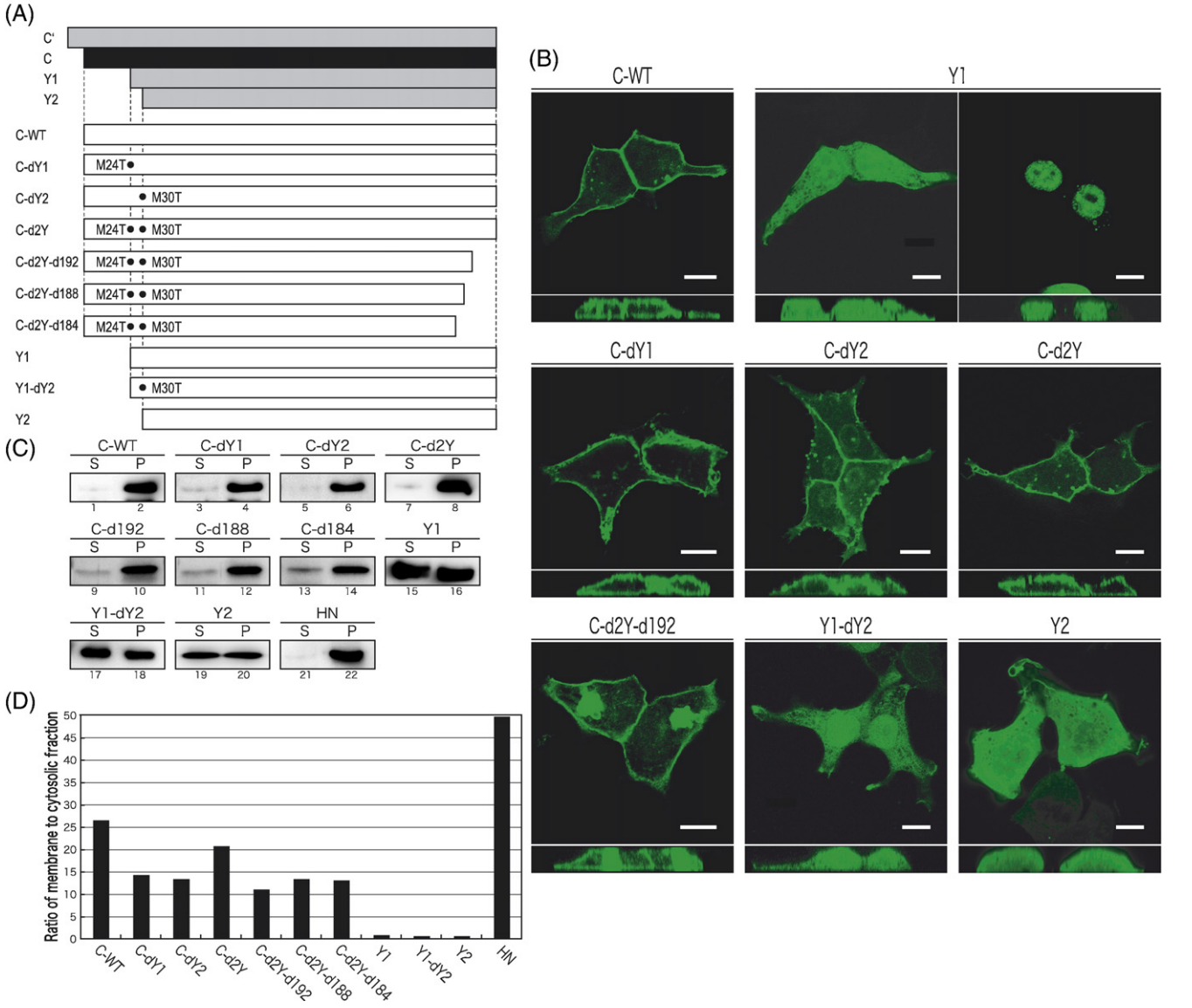

Fig. 1. Subcellular distributions of SeV C proteins. (A) Schematic representation of expression plasmids encoding C-WT, C-dY1, C-dY2, C-d2Y, C-d2Y-d192, C-d2Y-d188, C-d2Y-d184, Y1, Y1-dY2, and Y2. (B) C proteins were expressed in 293T cells. At 24 h p.t., cells were fixed with 3% formaldehyde, permeabilized with 0.1% Triton X-100, and stained with anti-C pAb and Alexa 488-conjugated anti-rabbit IgG antibody as primary and secondary antibodies, respectively. Cells were observed under a Zeiss LSM5 confocal microscope. The lower panels represent orthogonal views of the cells reconstituted from 20 slices. Bars, 10 μm. (C) C proteins were expressed in 293T cells, and cells were harvested at 24 h p.t. Cytosolic (S) and membrane fractions (P) were prepared from the PNS as described in Materials and methods, and equal amounts of each sample were separated by SDS-PAGE, and analyzed by Western blotting using anti-C pAb. A transmembrane protein, SeV hemagglutinin-neuraminidase (HN), was used as a control. (D) C proteins in the cytosolic and membrane fractions were quantitated using an LAS-1000 luminescent image analyzer. Ratios of the amounts of each C protein in the membrane fractions to those in the cytosolic fractions are shown.

budding (Irie et al., 2007; Sakaguchi et al., 2005; Sugahara et al., 2004). We next sought to determine whether the targeting of SeV C protein to the PM was important for this enhancement of budding. For this purpose, we first examined SeV M-VLP budding in the presence of the C mutants using a functional budding assay (Fig. 2). 293T cells were transfected with M-WT plasmid together with the designated C mutants. Almost identical amounts of M protein were expressed in transfected cells (Fig. 2A, lanes 13–22), and the expression of the C mutants was confirmed (Fig. 2A, lanes 25–33). Quantitation of the average amounts of radioactivity revealed that, consistently with our previous results (Sakaguchi et al., 2005), budding of SeV M-VLP was enhanced approximately 5-fold in the C-WT-transfected cells where C, Y1, as well as Y2 proteins were produced (Figs. 2A, lane 3, and B), although additional viral proteins, HN, F, and N, were not present, unlike in our previous report (Sakaguchi et al., 2005). Similar enhancement was also observed in the C-dY1-, C-dY2-, and C-d2Y-transfected cells where C and Y2, C and Y1, and C protein alone were expressed, respectively (Figs. 2A, lanes 4–6, and B). As expected from our previous results (Sakaguchi et al., 2005), such enhancement was not observed in the C-d2Y-d192, C-d2Y-d188, or C-d2Y-d184-transfected cells, where only the C-terminally-deleted C proteins but not Y1 and Y2 proteins were produced (Figs. 2A, lanes

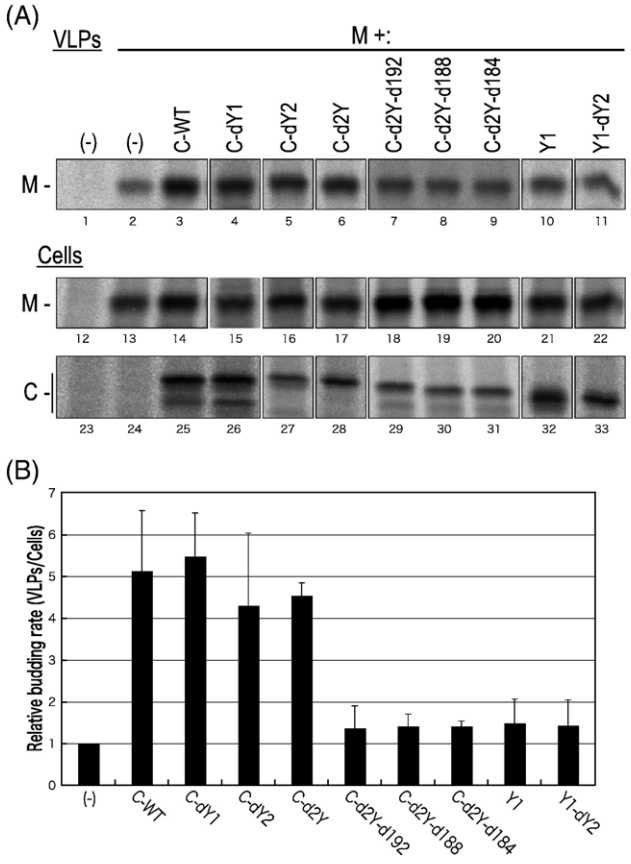

Fig. 2. Budding assay of SeV M-VLP in the presence of C mutants. (A) 293T cells were co-transfected with SeV M and the indicated C mutants. At 24 h p.t., cells were radio-labeled for another 6 h. Cell lysates and VLPs were immunoprecipitated with anti-SeV pAb for M protein and anti-C pAb for C mutants. (B) M proteins present in VLPs and cell lysates were quantitated. Budding rates were calculated as described in Materials and methods, and that from cells transfected with an empty vector (−) was set to 1. Bars represent the average from at least three independent experiments.

7–9, and B). In the Y1 or Y1-dY2-transfected cells where Y1 and Y2, or Y1 alone were produced, budding of SeV M-VLP was not essentially enhanced (Figs. 2A, lanes 10 and 11, and B). These results indicate that expression of the additional smaller Y1 and Y2 proteins is not required for the ability of the C protein to enhance SeV M-VLP budding, and that both the C- and N-terminal regions are important for this ability.

Since N-terminal deletion results in the loss of membrane association of the C protein (Fig. 1), the lack of ability of Y1 and Y1-dY2 proteins to enhance SeV M-VLP budding might have been due to their loss of targeting to the PM. To examine this possibility, the K-Ras CAAX domain, which is known to mediate PM association, were fused to the C-termini of C-d2Y and Y1-dY2. Three modified CAAX domains, 6KCVIM (KKKKKKCVIM), 12KCVIM (KKKKKKKKKKKKCVIM), and 6(KR)CVIM (KRKRKRKRKRKRCVIM), were chosen by referring to the previous report by Welman et al. (2000), and Y1-dY2-6KCVIM, -12KCVIM, and -6(KR)CVIM were generated (Fig. 3A). In the IFA study, fluorescence was observed at the PM and intracellular membrane structures in the cells transfected with any of these recombinants, unlike the fluorescence observed in the Y1 and Y1-dY2-tranfected cells where fluorescence was observed diffusely in the cytoplasm and the nucleus, although nuclear localization was still observed (Fig. 3B, middle, and data not shown). We decided to use Y1-dY2-6KCVIM for further experiments, because its PM localization was most predominant among these Y1-dY2-CAAX constructs (data not shown). We also introduced the modified 6KCVIM-type CAAX domain to the C-terminus of C-d2Y to generate C-d2Y-6KCVIM (Fig. 3A). In the IFA study, predominant PM localization was observed in cells transfected with this construct, like that observed in the cells transfected with C-d2Y and the other C mutants containing no N-terminal deletions (Fig. 3B, left). Furthermore, to examine whether the introduction of a heterologous Alix/AIP1-binding motif into the C-terminally-deleted C protein recombinants would recover the ability of budding enhancement, we generated C9 construct, in which an Alix/AIP1-interacting motif-containing region from EIAV p9Gag was fused to the N-terminus of the C-d2Y-d192 construct (Fig. 3A). In the IFA study, predominant PM localization was observed in the cells transfected with C9, like that observed in the cells transfected with the C-terminally-deleted C-d2Y-d192 (Fig. 3B, right). Predominant localization of the C-d2Y-6KCVIM, Y1-dY2-6KCVIM, and C9 proteins at the membrane was also confirmed by the subcellular fractionation analysis (Fig. 3C).

The effect of these recombinants on SeV M-VLP budding was also examined (Fig. 3D). Almost identical amounts of M protein were expressed in transfected cells (Fig. 3D, lanes 9–11 and 13–14), and the expression of the C mutants was confirmed (Fig. 3D, lanes 17, 18, and 21). Quantitation of the data revealed that budding of SeV M-VLP was enhanced approximately 5.5-fold in the presence of C-d2Y-6CVIM (compare bar graphs of Figs. 2 and 3D). Interestingly, enhancement of SeV M-VLP budding was also observed in the presence of Y1-dY2-6KCVIM and C9, although Y1-dY2 and C-d2Y-d192 failed to increase the budding efficiency (compare bar graphs of Figs. 2 and 3D).

These results indicate that the ability of SeV C protein to mediate PM association is important for its ability to enhance SeV M-VLP budding, and that the ability of budding enhancement can be recovered by the introduction of an Alix/AIP1-binding motif into the C-terminally-deleted C-d2Y-d192.

Alix/AIP1 is recruited to the PM by membrane-associating and Alix/AIP1-interacting C proteins

Since we previously reported that enhancement of SeV M-VLP budding by C protein correlates with SeV C-Alix/AIP1-interaction (Sakaguchi et al., 2005), the interaction of our C mutants with Alix/AIP1 was examined (Figs. 4 and 5). The interaction was first examined by co-immunoprecipitation analysis (Fig. 4). 293T cells were co-transfected with the indicated C mutants together with Alix/AIP1 and radio-labeled. For the C-terminal deletion mutants, C-d2Y-d192, -d188, and -d184, the interaction was examined by IP-Western blotting, because they were less efficiently radio-labeled probably due to their lower stability (Fig. 4B, and data not shown). Expression of adequate amounts of Alix/AIP1 and the C mutants was confirmed (Figs. 4A, lanes 1–24, and B, lanes 5–12). As expected from our previous results (Sakaguchi et al., 2005), Alix/AIP1 was co-immunoprecipitated with the C mutants, which

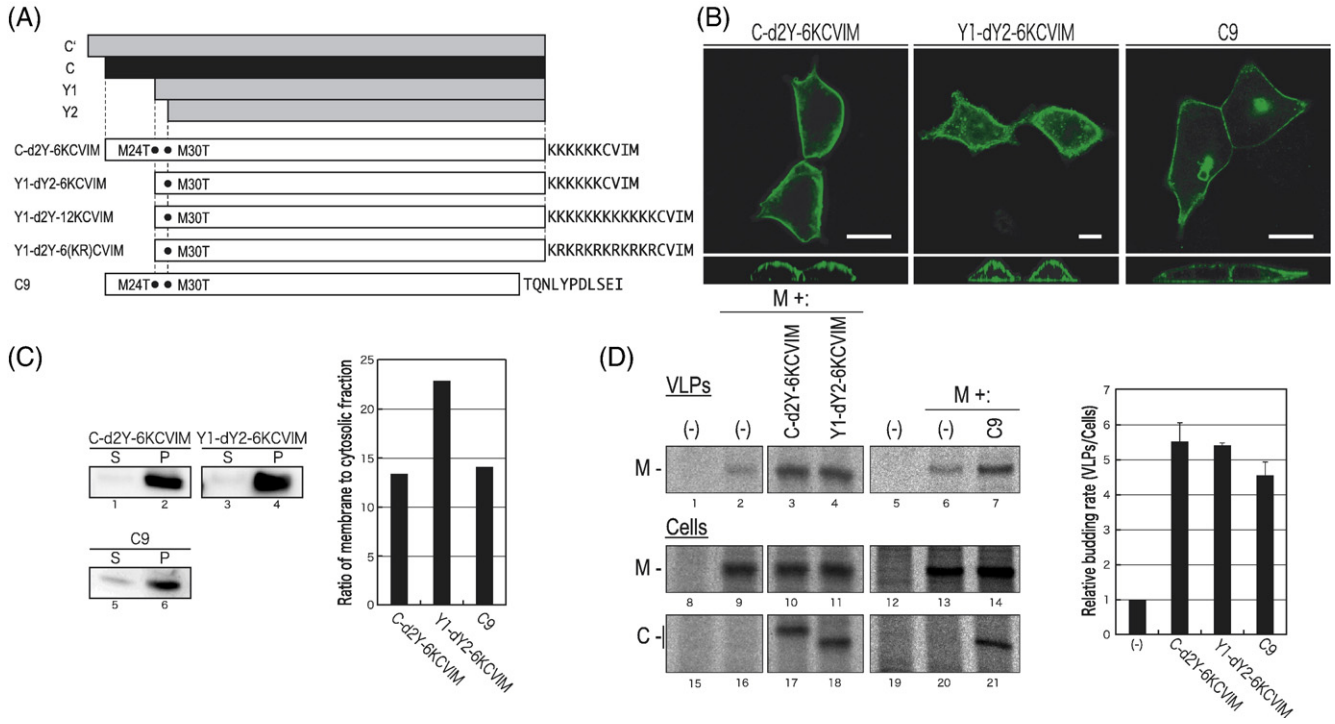

Fig. 3. Characteristics of the C mutants C-terminally fused with modified CAAX domains from K-Ras and Alix/AIP1-binding motif-containing region from EIAV p9 Gag. (A) Schematic representation of expression plasmids encoding C-d2Y-6KCVIM, Y1-dY2-6KCVIM, Y1-dY2-12KCVIM, Y1-dY2-6(KR)CVIM, and C9. (B) The indicated C mutants were subjected to immunofluorescence microscopy as shown in Fig. 1B. The lower panels represent orthogonal views of the cells reconstituted from 20 slices. Bars, 10 μm. (C) The mutant proteins present in the cytosolic and membrane fractions were analyzed by Western blotting as shown in Figs. 1C and D. (D) Budding assay of SeV M-VLPs in the presence of these C mutants. 293T cells co-transfected with SeV M and the indicated C mutants were radio-labeled, and analyzed as shown in Fig. 2. M proteins present in VLPs and cell lysates were quantitated. Budding rates were calculated as described in Materials and methods, and that from cells transfected with an empty vector (−) was set to 1. Bars represent the average from three independent experiments.

retained the intact C-terminus, including even Y1 and Y1-dY2, regardless of the presence or absence of the expression of additional smaller Y1 and/or Y2 proteins (Fig. 4A, lanes 4–9), but not with any of the C-terminally deleted C mutants (Fig. 4B, lanes 2–4). These results indicate that the C-terminal 12 amino acids of SeV C protein are important for the interaction with Alix/AIP1. Alix/AIP1 was also co-immunoprecipitated with C-d2Y-6KCVIM and Y1-dY2-6KCVIM, indicating that the 6KCVIM

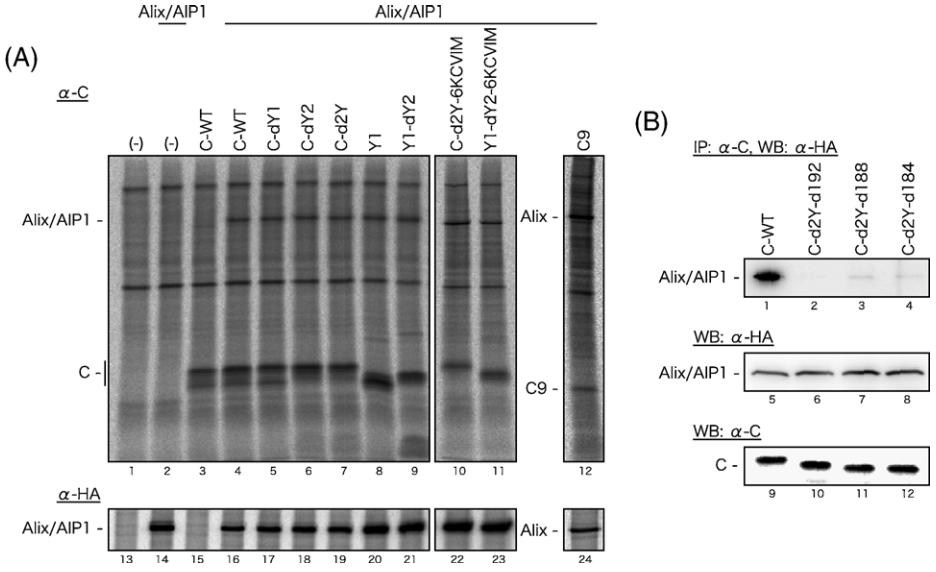

Fig. 4. Interaction between the C mutants and Alix/AIP1. 293T cells were co-transfected with 5′ HA-tagged Alix/AIP1 and the indicated C mutants. (A) At 24 h p.t., cells were radio-labeled, cell lysates were prepared, and immunoprecipitated with anti-C or anti-HA antibodies. The immunoprecipitates were separated by SDS-PAGE. (B) Interaction was also examined by IP-Western. At 24 h p.t., cell lysates were prepared, and immunoprecipitated with anti-C pAb. The immunoprecipitates were analyzed by Western blotting using anti-HA mAb to detect Alix/AIP1.

amino acid sequence attached to the C-termini of C-d2Y and Y1-dY2 did not abolish their binding with Alix/AIP1 (Fig. 4A, lanes 10–11). In addition, C9 also interacted with Alix/AIP1, indicating that the Alix/AIP1-binding activity of C-d2Y-d192 was recovered by introduction of the heterologous Alix/AIP1-binding region (Fig. 4A, lane 12).

We next examined SeV C-Alix/AIP1-interaction by immunofluorescence microscopy (Fig. 5A). 293T cells were co-transfected with the indicated C mutants together with Alix/AIP1. At 24 h p.t., cells were stained with anti-C and anti-HA antibodies as primary antibodies and Alexa 546-conjugated anti-rabbit IgG (red) and Alexa 488-conjugated anti-mouse IgG (green) antibodies as secondary antibodies, respectively. When Alix/AIP1 was expressed alone, fluorescence was observed diffusely throughout the cytoplasm (Fig. 5A, top). In the case of the co-transfection of Alix/AIP1-interacting C-d2Y and Alix/AIP1, C-d2Y was predominantly localized at the PM, and Alix/AIP1 was now also predominantly found and co-localized at the PM with C-d2Y (Fig. 5A, second from the top). A similar result was observed in the cells co-transfected with C-d2Y-6KCVIM and Alix/AIP1 (Fig. 5A, fourth from the top). In contrast, in the case of co-transfection of Alix/AIP1-non-interacting C-d2Y-d192 and Alix/AIP1, Alix/AIP1 was still observed diffusely in the cytoplasm, and did not co-localize at the PM, although C-d2Y-d192 was predominantly found at the PM (Fig. 5A, third from the top). In the case of co-transfection with Alix/AIP1-interacting Y1-dY2 and Alix/AIP1, no PM localization was observed for either Y1-dY2 or Alix/AIP1, and co-localization in the cytoplasm was observed (Fig. 5A, third from the bottom). In contrast, in the cells co-transfected with Alix/AIP1-interacting Y1-dY2-6KCVIM or C9 and Alix/AIP1, the co-localization was now observed at the PM and the intracellular membranes (Fig. 5A, second and first from the bottom).

Furthermore, we examined subcellular localization of Alix/AIP1 in the presence of the recombinant C proteins used in Fig. 5A by the subcellular fractionation analysis (Figs. 5B and C). Ratios of Alix/AIP1 detected in the membrane fraction to that in the cytosolic fraction were increased by 2–3.3-fold in the presence of the PM-associating and Alix/AIP1-interacting C proteins, such as C-d2Y, C-d2Y-6KCVIM, Y1-dY2-6KCVIM, and C9, compared to that in the cells transfected with Alix/AIP1 alone, whereas the ratios were not changed in the presence of Y1-d2Y and C-d2Y-d192, lacking PM-association and Alix/AIP1-interaction, respectively (Fig. 5C).

Together with the results described above, these results indicate that the C proteins retaining both the ability to associate with the PM and the ability to interact with Alix/AIP1 are able to recruit Alix/AIP1 to the PM and to enhance SeV M-VLP budding.

Alix/AIP1 co-localizes with SeV M protein at the PM

Since we recently reported that SeV M protein also functionally interacts with Alix/AIP1 (Irie et al., 2007), interaction of M and Alix/AIP1 was examined by immunofluorescence microscopy (Fig. 5D). 293T cells were co-transfected with SeV M together with Alix/AIP1 or an empty plasmid. At 24 h p.t., cells were stained with anti-SeV and anti-HA antibodies as primary antibodies and Alexa 546-conjugated anti-rabbit IgG (red) and Alexa 488-conjugated anti-mouse IgG (green) antibodies as secondary antibodies, respectively. When SeV M was expressed alone, fluorescence was observed not only throughout the cytoplasm but also at the cell periphery (Fig. 5D, top). In the case of co-transfection of SeV M and Alix/AIP1, co-localization of SeV M and Alix/AIP1 was observed at the cell periphery, although both proteins were observed also at the cytoplasm without co-localizing (Fig. 5D, bottom).

VPS4A-dependent SeV M-VLP budding requires recruitment of Alix/AIP1 by SeV C protein

It is known that Alix/AIP1 is a component of MVB sorting machinery (Katoh et al., 2004, 2003), and we previously reported that SeV budding was sensitive to DN VPS4A expression (Sakaguchi et al., 2005). We next examined the effect of overexpression of DN VPS4A on SeV M-VLP budding in the presence or absence of the C mutants using a functional VLP budding assay (Fig. 6). The expression of adequate amounts of WT and DN VPS4A (VPS4-WT and VPS4-EQ, respectively) and the C mutants was confirmed in the transfected cells (Fig. 6A, lanes 43–84). In the absence of additional C proteins, budding of SeV M-VLP was reduced approximately 5-fold even by overexpression of VPS4-WT, but a further decrease was not observed in the cells receiving VPS4-EQ (Figs. 6A, lanes 1–3, and B). Similar results were observed in the presence of C-d2Y-d192, Y1, and Y1-d2Y, neither of which recruited Alix/AIP1 to the PM; SeV M-VLP budding was not further reduced by VPS4-EQ, compared to that in the cells receiving VPS4-WT, although the VLP budding was reduced even by VPS4-WT expression, compared to that in the empty-vector-transfected cells (Figs. 6A, lanes 7–12, B, and data not shown). In contrast, interestingly, SeV M-VLP budding was increased approximately 2-fold by VPS4-WT expression in the presence of C-d2Y possessing the ability to recruit Alix/AIP1 to the PM, compared to that observed in the empty-vector-transfected sample, and was decreased approximately 10-fold by VPS4-EQ overexpression compared to that observed in the cells receiving VPS4-WT (Figs. 6A, lanes 4–6, and B). Similar results were observed in the presence of C-WT and C-d2Y-6KCVIM, which also possess the ability to recruit Alix/AIP1 to the PM (Figs. 6A, lanes 13–15, B, and data not shown). In addition, in the presence of Y1-dY2-6KCVIM and C9, which were able to recruit Alix/AIP1 to the PM, budding of SeV M-VLP was sensitive to VPS4-EQ, and was reduced approximately 7- and 9-fold, respectively, by overexpression of VPS4-EQ compared to that observed in the cells receiving VPS4-WT (Figs. 6A, lanes 16–21, and B).

These results strongly suggest that SeV M-VLPs bud through the use of cellular machinery dependent on VPS4A activity only when Alix/AIP1 is recruited to the PM by SeV C protein, although budding of SeV M-VLP does not seem dependent on VPS4A in the absence of the C protein.

It should be noted that, in this experiment, M protein expression in the cells was reduced by both VPS4-WT and VPS4-EQ expression, compared to that in the empty-vector-transfected sample, probably due to the cytotoxic effect by overexpression of

these VPS4 proteins (Fig. 6A, lanes 22–42). This difference of M protein expression between the empty vector- and VPS4 constructs-transfected samples might lead incorrect conclusions. However, the results in Fig. 6 were highly reproducible, and most importantly, the difference in sensitivity of SeV M-VLP budding to the DN VPS4 expression between in the presence and the

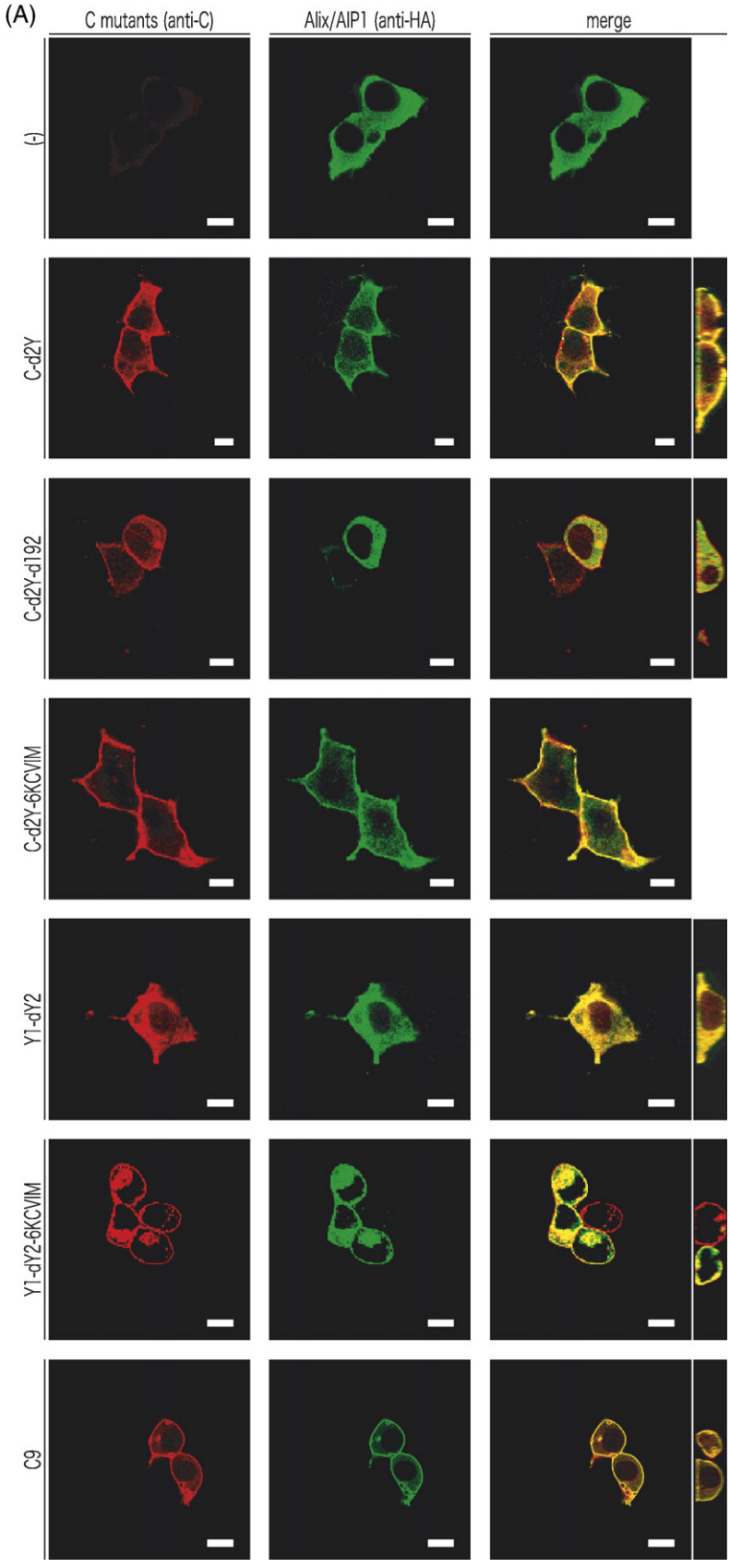

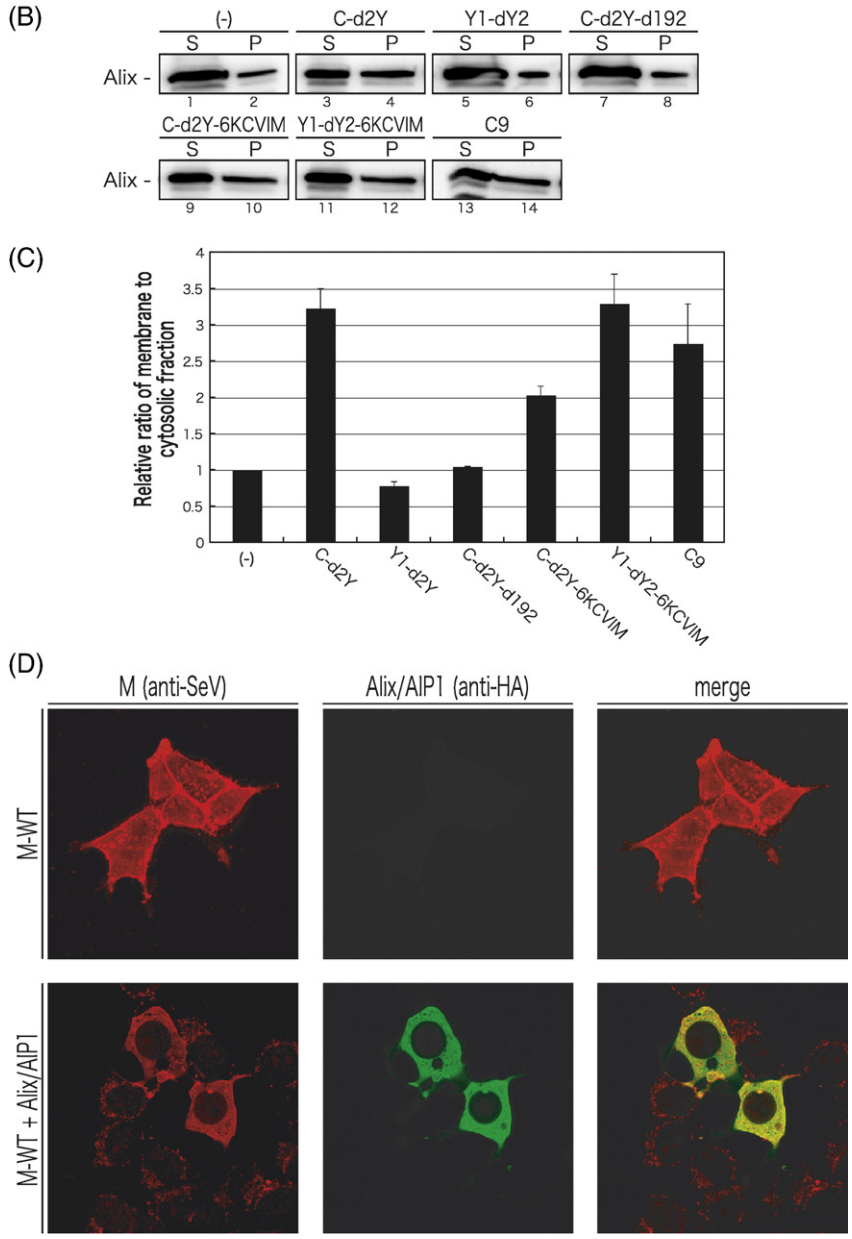

Fig. 5. (A) Confocal microscopy for 293T cells co-transfected with the C mutants and Alix/AIP1. At 24 h p.t., cells were stained with anti-C (red) and anti-HA (green) antibodies. The right panels of each row represent orthogonal views of the cells reconstructed from 20 slices. Bars, 10 μm. (B) Alix/AIP1 present in the cytosolic and membrane fractions prepared from the cells co-transfected with Alix/AIP1 with the indicated C mutants or an empty vector (−) was analyzed by Western blotting using anti-HA mAb. (C) Alix/AIP1 in the cytosolic and membrane fractions were quantitated as shown in Fig. 1D. Ratios of the amounts of Alix/AIP1 in the membrane fraction to that in the cytosolic fraction were calculated and that from the cells co-transfected with the empty vector was set to 1. Bars represent the average from at least three independent experiments. (D) Confocal microscopy for 293T cells co-transfected with SeV M and Alix/AIP1 proteins. At 24 h p.t., cells were stained with anti-SeV (red) and anti-HA (green) antibodies.

absence of the PM-associating and Alix/AIP1-interacting C proteins was observed, although the levels of M protein expression in the cells receiving VPS4-WT and VPS4-EQ were equivalent.

SeV M-VLP budding was inhibited by overexpression of DN CHMP4B regardless of the presence or absence of the C proteins

It is known that CHMP4B (chromatin-modifying protein 4b; charged multivesicular body protein 4b) is a component of MVB sorting machinery and interacts with Alix/AIP1 (Katoh et al., 2003), that CHMP4B recombinants which were N- or C-terminally fused with fluorescent proteins, such as GFP and YFP, show DN phenotype (Howard et al., 2001), and that the DN CHMP4B inhibits budding of the retroviruses possessing Alix/AIP1-interacting L-domain motifs (Fisher et al., 2007; von Schwedler et al., 2003). In addition, we previously reported that both SeV M and C proteins interact with Alix/AIP1 and that both these interactions were important for M-VLP budding (Irie et al., 2007; Sakaguchi et al., 2005). Finally, we examined the effect of GFP-CHMP4B overexpression on SeV M-VLP budding in the presence or absence of the C proteins using a functional budding assay (Fig. 7). Almost identical amounts of M protein were expressed in transfected cells

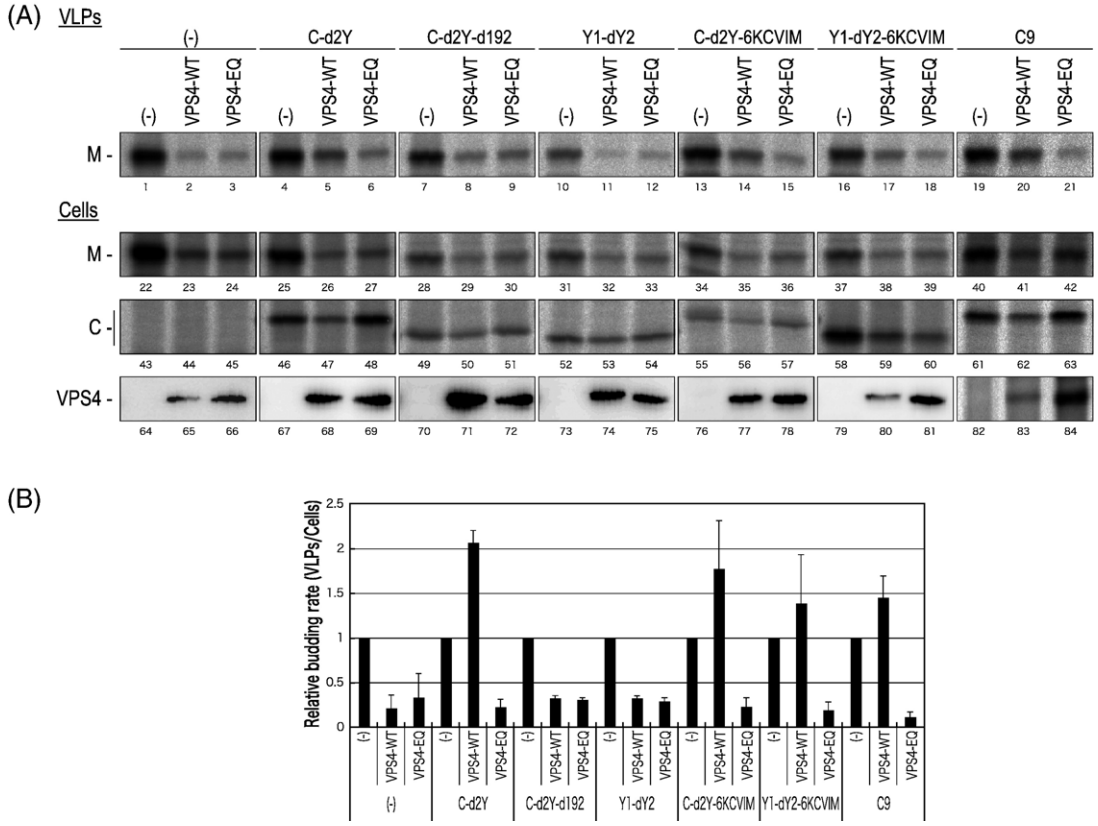

Fig. 6. Effect of overexpression of DN VPS4A on SeV M-VLP budding in the presence or absence of the C mutants. (A) 293T cells were co-transfected with SeV M and the indicated C mutants together with either an empty vector (−), VPS4-WT, or VPS4-EQ. At 24 h p.t., cells were radio-labeled for another 6 h. Cell lysates and VLPs were immunoprecipitated with anti-SeV pAb for M protein, anti-C pAb for C mutants, or anti-GFP pAb for VPS4A mutants. (B) M protein present in VLPs and cell lysates was quantitated. Budding rates were calculated as described in Materials and methods, and that from the cells receiving no VPS4 plasmids (−) was set to 1. Bars represent the average from at least three independent experiments.

(Fig. 7, lanes 7–12), and the expression of the C mutants and GFP-CHMP4B was confirmed (Fig. 7, lanes 13–24). Budding of SeV M-VLP was more than 5-fold reduced in the EGFP-CHMP4B-transfected cells compared to that in the cells receiving the empty-EGFP vector regardless of the presence or absence of the C proteins (Fig. 7). This result suggests that SeV M-VLP budding is inhibited by disruption of Alix/AIP1 activity by overexpression of EGFP-CHMP4B regardless of the presence or absence of the C protein, and supports the importance of Alix/AIP1 in the VLP budding.

Discussion

Our understanding of the budding of enveloped viruses has been dramatically increased since L-domain motifs were identified within viral matrix and retroviral Gag proteins. Most of enveloped viruses are believed to commonly utilize cellular MVB sorting machinery for efficient virus budding, because the major types of L-domain motifs have been reported to interact with cellular factors, which are known to be components of ESCRTs and/or have been shown to have some link to MVB sorting machinery (Bieniasz, 2006; Demirov and Freed, 2004) and budding of retroviruses possessing any of the major types of L-domain motifs is inhibited by overexpression of DN forms of VPS4A (Demirov and Freed, 2004).

In contrast, for many enveloped viruses, the mechanism of efficient virus budding is still unclear, and no L-domain motifs have been identified. For paramyxoviruses, the mechanisms of viral and VLP budding remain to be determined, although FPIV, YMYL, and YLDL sequences within the M proteins of SV5, Nipah virus, and SeV, respectively, have recently been reported to be critical for VLP budding (Ciancanelli and Basler, 2006; Irie et al., 2007; Schmitt et al., 2005). Budding of SV5 M-VLPs is inhibited by DN VPS4 overexpression, but the interacting partner has not been identified yet (Schmitt et al., 2005). For Nipah virus, both the cellular proteins interacting with the YMYL motif and whether the MVB sorting machinery is involved in VLP budding are unclear (Ciancanelli and Basler, 2006). We recently reported that SeV M protein functionally interacts with Alix/AIP1 via its YLDL motif, and that SeV budding is sensitive to DN VPS4 expression (Irie et al., 2007; Sakaguchi et al., 2005).

We previously reported that SeV was unique in that one of the viral accessory proteins, C, enhanced M-VLP budding in a C-Alix/AIP1-interaction-dependent manner, although SeV M protein drives budding, like in other enveloped viruses (Irie et al., 2007; Sakaguchi et al., 2005; Sugahara et al., 2004). Recently, C protein was shown to associate with the PM in the experiments using an artificial recombinant C protein in which the N-terminal 23 amino acids and the remaining portion were separated by inserting a

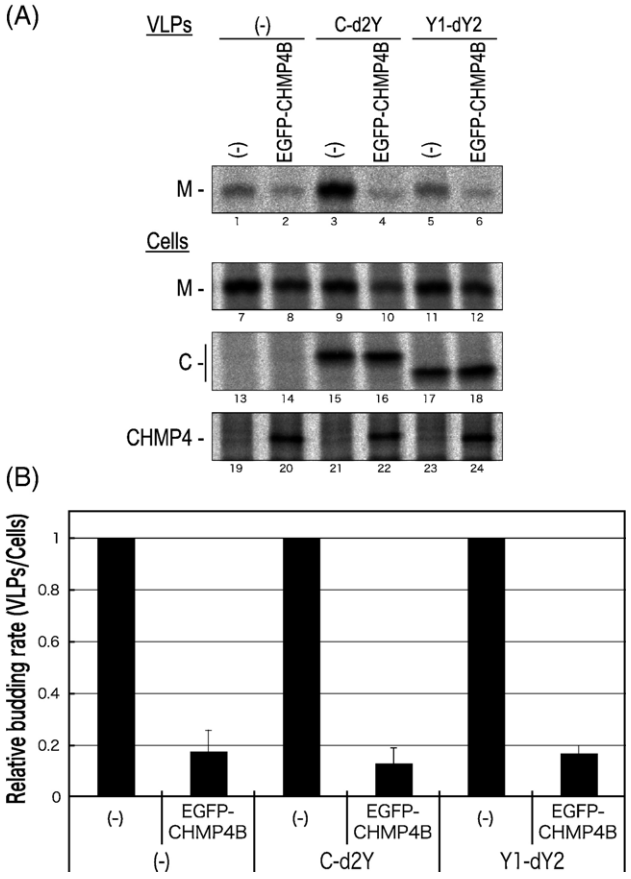

Fig. 7. Effect of overexpression of EGFP-CHMP4B on SeV M-VLP budding in the presence or absence of the C mutants. (A) 293T cells were co-transfected with SeV M and the indicated C mutants together with either an empty EGFP vector (−), or EGFP-CHMP4B. At 24 h p.t., cells were radio-labeled for another 6 h. Cell lysates and VLPs were immunoprecipitated with anti-SeV pAb for M protein, anti-C pAb for C mutants, or anti-GFP pAb for EGFP-CHMP4B. (B) M protein present in VLPs and cell lysates was quantitated. Budding rates were calculated as described in Materials and methods, and that from the cells receiving empty EGFP plasmid (−) was set to 1. Bars represent the average from at least three independent experiments.

reporter tdTomato fluorescent protein, and this function was mapped to the N-terminal 23 amino acids (Marq et al., 2007). In this report, we show that the intact SeV C protein was able to localize predominantly at the PM without additional smaller Y1 and/or Y2 protein expression (Fig. 1). Interestingly, however, in the C-dY2-transfected cells where C and Y1 proteins were produced, fluorescence was observed at the nuclear envelope as well as the PM, and in the cells transfected with C-dY1, C-dY2, and C-d2Y lacking Y2, Y1, and both Y1 and Y2 expression, respectively, more localization at intracellular membrane structures appeared than in the C-WT-transfected cells (Fig. 1). In addition, in the Y1- and Y1-dY2-transfected cells where Y1 and Y2, and Y1 alone were produced, respectively, nuclear as well as cytoplasmic localization was observed, although in the C-WT and C-dY1-transfected cells where Y1 and/or Y2 as well as C proteins were produced, such localization at the nuclear envelope and in the nucleus was not observed (Fig. 1). These observations suggest that C, Y1, and Y2 proteins may coordinate their subcellular localization with each other to play different roles in the viral life cycle. It will be of interest to determine the contributions of these C proteins to various functions of C proteins in the viral life cycle.

We also found that the PM-associating and Alix/AIP1-interacting C proteins were able to enhance M-VLP budding, but the PM-non-associating and/or Alix/AIP1-non-interacting C proteins were not (Figs. 1–4). Indeed, Alix/AIP1 was recruited to the PM only when the PM-associating and Alix/AIP1-interacting C proteins were co-expressed, and such C proteins were able to enhance M-VLP budding (Fig. 5). In contrast, Alix/AIP1 was predominantly localized in the cytoplasm in the presence of the C proteins lacking the ability of PM-association and/or Alix/AIP1-interaction, and such C proteins failed to enhance M-VLP budding (Fig. 5). For example, C-d2Y-d192, retaining PM-association but lacking Alix/AIP1-interaction, no longer recruited Alix/AIP1 to the PM and enhanced M-VLP budding. Interestingly, this ability of C protein to enhance M-VLP budding could be recovered by fusing a modified CAAX domain from K-Ras to the C-terminus of Y1-d2Y protein, which originally retained Alix/AIP1-interaction, but lacked PM-association (Figs. 3 and 5). In addition, the budding enhancement was also recovered by fusing an Alix/AIP1-binding motif-containing region from EIAV p9 Gag to the C-terminus of C-d2Y-d192 protein, which originally retained PM-association, but lacked Alix/AIP1-interaction (Figs. 3 and 5).

Surprisingly, M-VLP budding was not sensitive to overexpression of DN VPS4, in the absence of any additional viral proteins (Fig. 6), although we recently reported that M protein functionally interacts with Alix/AIP1 (Irie et al., 2007), and that SeV budding is reduced by DN VPS4A expression (Sakaguchi et al., 2005). Similar observation was recently reported by Gosselin-Grenet et al. (2007). M-VLP budding was also insensitive to DN VPS4 when the C mutants deficient in enhancement of M-VLP budding, such as C-d2Y-d192, Y1, and Y1-dY2, were co-transfected (Fig. 6). Interestingly, however, budding of M-VLP now became sensitive to DN VPS4 expression in the presence of the PM-associating and Alix/AIP1-interacting C mutants; M-VLP budding was reduced approximately 10-fold in the case of DN VPS4 overexpression compared to that observed in the cells receiving VPS4-WT (Fig. 6).

In addition, SeV M-VLP budding was reduced by EGFP-CHMP4B expression regardless of the presence and the absence of C protein expression (Fig. 7). This result supports our previous observations that both M-Alix/AIP1 and C-Alix/AIP1-interactions are important for efficient M-VLP budding (Irie et al., 2007; Sakaguchi et al., 2005), because EGFP-CHMP4B abolishes Alix/AIP1 function by direct binding, although budding of VLPs formed by M protein alone seems to be independent of the cellular MVB sorting function.

In sum, we propose a hypothetical model for SeV M-VLP budding (Fig. 8). M protein itself has the ability to associate with the inner surface of the PM and aggregates via M–M interaction at the budding site (Fig. 8, pathway 1) (Bachi, 1980; Mottet et al., 1996; Stricker et al., 1994). C protein is also targeted to the PM by its own PM targeting signal (Fig. 8, pathway 4) (Marq et al., 2007). A part of C protein recruits Alix/AIP1 to the PM by physical interaction (Fig. 8, pathway 3) (this report). Since Alix/AIP1 is a component of the ESCRT machinery (Katoh et al., 2003), this machinery may also be recruited to the PM, and is

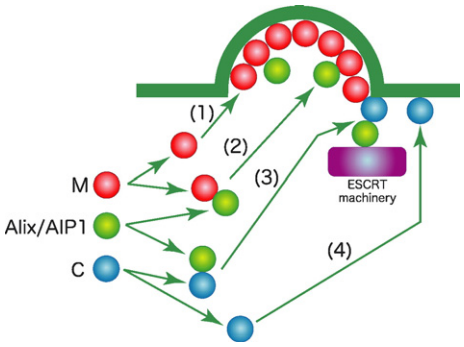

Fig. 8. Possible model for SeV M-VLP budding (see text).

now utilized for efficient M-VLP budding. As we reported previously that M protein was also able to physically interact with Alix/AIP1 (Irie et al., 2007), a part of M protein also interacts with Alix/AIP1 at the PM (Figs. 8, pathway 2, and 5D). In this model, it still remains to be determined whether C protein recruits Alix/AIP1 to the site where M protein aggregates and M-VLP budding occurs. The interaction between M and C proteins has not been reported and has not been detected Co-IP experiments (data not shown). As described above, M protein alone is able to bud from the cell surface in a VPS4 activity-independent manner, although M-VLP budding is sensitive to DN VPS4 expression, like SeV budding, in the presence of the C proteins with the ability to recruit Alix/AIP1 to the PM. Alix/AIP1 is not only a component of MVB sorting machinery, but also has the ability to generate an MVB-resembling membrane structure *in vitro* in the presence of a specific phospholipid, lysobisphosphatidic acid, and to form exosomes, small membrane structures that are liberated from cells (Matsuo et al., 2004; Thery et al., 2001). Such functions of Alix/AIP1 itself may contribute to increasing the efficiency of VLP budding formed by M protein alone. Recently, HIV-1 Nef was reported to interact with Alix/AIP1, resulting in the proliferation of MVBs and enhancement of budding efficiency, in addition to the interaction of Gag with Tsg101 and Alix/AIP1 via its PTAP and LxxL motifs, respectively (Costa et al., 2006). Experiments to determine how Alix/AIP1 contribute to M-VLP budding in the absence of other viral proteins are currently under way.

Finally, it seems that L-domain functions are not critical to the budding of some viruses. For example, it has been reported that release of recombinant VSVs and Ebola viruses whose L-domain motifs are knocked out is reduced by 1–2 logs, but still 10^6–10^7 pfu/ml of the viruses are released into the culture medium (Irie and Harty, 2005; Irie et al., 2005, 2004a; Jayakar et al., 2000; Neumann et al., 2005). In addition, unlike PPxY-type L-domain-containing retroviruses, budding of the PPxY motif-containing rhabdoviruses and that of an Ebola VP40 mutant, VP40-dPTA, in which only the PPEY motif was retained but the PTAP motif was abolished by deleting the first three amino acids of the overlapping motifs, was not sensitive to DN forms of VPS4 (Irie et al., 2004b). These observations imply that the major budding force of the matrix protein is provided by mechanisms other than the MVB sorting pathway, and that the viruses utilize the cellular MVB sorting machinery just to increase the efficiency of virus budding. For most L-domain-containing viruses, their matrix or Gag proteins possess both of these two functions, driving budding and increasing budding efficiency. In contrast, in the case of SeV, these functions seem to be separated into two viral proteins M and C: M protein drives budding and C protein increases budding efficiency. This makes SeV a useful tool for seeking a better understanding of envelope virus budding.

In some cases, viral L-domains and cellular MVB sorting machinery contributed minimally in virus replication, although critical for VLP budding. For example, a p6-deficient HIV-1 recombinant was able to be released as efficiently as a wt virus and was not sensitive to expression of a DN form of VPS4, when an activity of viral protease was abolished by introducing a specific amino acid change or adding a specific inhibitor (Fang et al., 2007). For SeV, in contrast to our observations in the SeV M-VLP system (Irie et al., 2007; Sakaguchi et al., 2005), neither expression of DN VPS4 nor depletion of Alix/AIP1 largely affected virus replication (Gosselin-Grenet et al., 2007). In addition, inhibition of C protein expression by a siRNA technique did not affect the recombinant SeV lacking expression of C proteins from P mRNA but expressing GFP-fused C protein from an additional cistron. However, we previously reported that SeV budding from the cells transfected with purified SeV nucleocapsid is sensitive to DN VPS4 (Sakaguchi et al., 2005), and we found that knock-out of C' and C protein expression from P mRNA resulted in reduced SeV budding (data not shown). Such discrepancies might be due to the difference in experimental system used, and these observations suggest that virus budding is a more complicated event especially than VLP budding, and that more viral and cellular factors involved in virus budding are still unidentified.

Materials and methods

Cells and antibodies

Human 293T cells were maintained in Dulbecco's minimum essential medium (DMEM; Sigma) supplemented with 10% fetal bovine serum (FBS; Biological Industries, Kibbutz Beit Haemek, Israel) and penicillin–streptomycin (Invitrogen) at 37 °C. Polyclonal antibodies (pAb) against the whole virion of SeV was described previously (Sugahara et al., 2004). pAb against SeV C protein was kindly provided by A. Kato (National Institute for Infectious Diseases, Japan). pAb against green fluorescent protein (GFP) (sc-8334; Santa Cruz biotechnology, Santa Cruz, CA) and monoclonal antibody (mAb) against HA-tag (HA.C5; GeneTex, San Antonio, TX) were used according to the protocols of the suppliers.

Plasmid construction

Plasmids encoding SeV C-WT, SeV HN, and 5′ HA-tagged AIP1-WT in pCAGGS.MCS vector and a plasmid encoding SeV Y2 in pKS vector have been described previously (Sakaguchi et al., 2005; Sugahara et al., 2004). C gene mutants (C-dY1, C-dY2, C-d2Y, C-d2Y-d192, C-d2Y-d188, C-d2Y-d184, Y1, and Y1-dY2) and the other mutants [C-d2Y-6KCVIM, Y1-dY2-6KCVIM, Y1-dY2-12KCVIM, Y1-dY2-6(KR)CVIM, and C9] were generated

by introducing point-mutations using a QuickChange XL site-directed mutagenesis kit (Stratagene) and using a standard PCR technique, respectively, and inserted into the pCAGGS.MCS vector. The full-length cDNA clone of human CHMP4B (DDBJ/EMBL/GenBank accession number BC033859) was obtained from Open Biosystems and subcloned into pEGFP-C1 vector (Clontech). All of these constructs were confirmed by DNA sequencing. Plasmids encoding EGFP-fused VPS4A-WT and a DN mutant VPS4A-E228Q were kindly provided by W. Sundquist (University of Utah).

Immunofluorescence microscopy

Human 293T cells cultured in 6-well plates containing glass coverslips were transfected with the indicated plasmids using the FuGENE HD transfection reagent (Roche Diagnostics). At 24 h post-transfection (p.t.), cells were fixed with 3% formaldehyde solution, and then treated with 0.1% Triton X-100 in phosphate-buffered saline (PBS). Cells were then stained using anti-C pAb or anti-SeV pAb, and/or anti-HA mAb as primary antibodies and Alexa 488- or Alexa 546-conjugated anti-rabbit IgG goat pAb and/or Alexa 488-conjugated anti-mouse IgG goat pAb (Invitrogen) as secondary antibodies, respectively. Coverslips were mounted on glass slides and observed using a Zeiss LSM 5 confocal microscope (Carl Zeiss).

Subcellular fractionation

293T cells cultured in 10 cm dishes were transfected with the indicated plasmids using the FuGENE HD reagent. At 24 h p.t., subcellular fractions were prepared as described previously by Welman et al. (2000). Briefly, cells were washed with ice-cold PBS, resuspended in 1 ml of ice-cold hypotonic buffer (10 mM HEPES [pH 7.5], 10 mM NaCl, 1 mM $MgCl_2$, 1 mM $CaCl_2$, 1 mM KCl) containing "Complete" protease inhibitor cocktail (Roche Diagnostics), incubated on ice for 15 min, and homogenized by 25 passages through a $25G^5/_8$ (0.5×16) needle. After centrifugation for 5 min at $500\times g$, postnuclear supernatant (PNS) was centrifuged for 30 min at $120{,}000\times g$. The pellet (membrane fraction) was suspended in 100 μl of SDS-PAGE sample buffer (125 mM Tris–HCl [pH 6.8], 4.6% sodium dodecyl sulfate [SDS], 5% 2-mercaptoethanol, 0.005% bromophenol blue, 20% glycerol). The supernatant (soluble fraction) was subjected to acetone precipitation, and the protein pellet was suspended in 100 μl of SDS-PAGE sample buffer. Equal volumes of each fraction sample were analyzed by 12% SDS-PAGE followed by Western blotting using anti-SeV pAb, anti-C pAb, or anti-HA mAb. Protein bands were detected by a chemiluminescent method using an ECL plus Western blotting detection reagent (GE Healthcare Life Sciences), and analyzed using an LAS-1000 luminescent image analyzer (Fuji Film).

Functional VLP budding assay

293T cells cultured in 6-well plates were transfected with the indicated plasmids using the FuGENE HD reagent. At 24 h p.t., cells were metabolically labeled with 3.7 MBq/ml of [^{35}S]Met-Cys (Pro-mix; GE Healthcare Life Sciences) for 6 h. Culture medium was harvested and clarified at 3,000 rpm for 10 min. The supernatant was then centrifuged at 40,000 rpm for 2 h through a 20% sucrose cushion. The pellet was suspended in radioimmunoprecipitation assay (RIPA) buffer (1% Triton X-100, 1% sodium deoxycholate, 0.1% SDS, 10 mM Tris–HCl [pH 7.4], 150 mM NaCl) containing a "Complete" protease inhibitor cocktail, immunoprecipitated with anti-SeV pAb, and analyzed by SDS-PAGE. In order to examine the protein expression from transfected plasmids, cell lysates were also immunoprecipitated with the appropriate antibodies, and analyzed by SDS-PAGE. Protein bands were visualized and quantitated with a BAS2000 Bio-imaging analyzer (Fuji Film). VLP budding rate was calculated as the ratio of M protein in VLPs to that in cell lysates. Samples from the cells transfected with an empty pCAGGS.MCS vector were used as the background control.

Co-IP

293T cells cultured in 6-well plates were co-transfected with the indicated plasmids using the FuGENE HD reagent, and metabolically labeled with [^{35}S]Met-Cys as described above. Cells were then suspended in cell lysis buffer (0.5% NP-40, 20 mM Tris–HCl [pH 7.4], 150 mM NaCl) containing a "Complete" protease inhibitor cocktail. Cell lysate samples were immunoprecipitated with either anti-C or -HA antibody. The immunoprecipitates were separated by SDS-PAGE, and analyzed with a BAS2000 Bio-imaging analyzer.

IP-Western

293T cells cultured in 6-well plates were co-transfected with the indicated plasmids using the FuGENE HD reagent. At 24 h p.t., cells were suspended in cell lysis buffer as described above. Cell lysate samples were immunoprecipitated with anti-C pAb, and the immunoprecipitates were separated by SDS-PAGE followed by Western blotting using anti-HA mAb to detect co-immunoprecipitated HA-tagged Alix/AIP1. Cell lysates were also subjected directly to Western blotting using anti-C or anti-HA antibody to confirm the expression of C mutants and Alix/AIP1, respectively.

Acknowledgments

We would like to thank the staff of the Research Center for Molecular Medicine and the Analysis Center of Life Science, Hiroshima University for the use of their facilities. This work was supported by Grants-in-Aid for Scientific Research from the Japan Society of the Promotion of Science.

References

Babst, M., Sato, T.K., Banta, L.M., Emr, S.D., 1997. Endosomal transport function in yeast requires a novel AAA-type ATPase, Vps4p. EMBO J. 16 (8), 1820–1831.

Babst, M., Wendland, B., Estepa, E.J., Emr, S.D., 1998. The Vps4p AAA ATPase regulates membrane association of a Vps protein complex required for normal endosome function. EMBO J. 17 (11), 2982–2993.

Babst, M., Katzmann, D.J., Estepa-Sabal, E.J., Meerloo, T., Emr, S.D., 2002a. Escrt-III: an endosome-associated heterooligomeric protein complex required for MVB sorting. Dev. Cell 3 (2), 271–282.

Babst, M., Katzmann, D.J., Snyder, W.B., Wendland, B., Emr, S.D., 2002b. Endosome-associated complex, ESCRT-II, recruits transport machinery for protein sorting at the multivesicular body. Dev. Cell 3 (2), 283–289.

Bachi, T., 1980. Intramembrane structural differentiation in Sendai virus maturation. Virology 106 (1), 41–49.

Bieniasz, P.D., 2006. Late budding domains and host proteins in enveloped virus release. Virology 344 (1), 55–63.

Ciancanelli, M.J., Basler, C.F., 2006. Mutation of YMYL in the Nipah virus matrix protein abrogates budding and alters subcellular localization. J. Virol. 80 (24), 12070–12078.

Costa, L.J., Chen, N., Lopes, A., Aguiar, R.S., Tanuri, A., Plemenitas, A., Peterlin, B.M., 2006. Interactions between Nef and AIP1 proliferate multivesicular bodies and facilitate egress of HIV-1. Retrovirology 3, 33.

Curran, J., Marq, J.B., Kolakofsky, D., 1992. The Sendai virus nonstructural C proteins specifically inhibit viral mRNA synthesis. Virology 189 (2), 647–656.

Demirov, D.G., Freed, E.O., 2004. Retrovirus budding. Virus Res. 106 (2), 87–102.

Fang, Y., Wu, N., Gan, X., Yan, W., Morrell, J.C., Gould, S.J., 2007. Higher-order oligomerization targets plasma membrane proteins and HIV Gag to exosomes. PLoS Biol. 5 (6), e158.

Fisher, R.D., Chung, H.Y., Zhai, Q., Robinson, H., Sundquist, W.I., Hill, C.P., 2007. Structural and biochemical studies of ALIX/AIP1 and its role in retrovirus budding. Cell 128 (5), 841–852.

Garcin, D., Latorre, P., Kolakofsky, D., 1999. Sendai virus C proteins counteract the interferon-mediated induction of an antiviral state. J. Virol. 73 (8), 6559–6565.

Garcin, D., Curran, J., Itoh, M., Kolakofsky, D., 2001. Longer and shorter forms of Sendai virus C proteins play different roles in modulating the cellular antiviral response. J. Virol. 75 (15), 6800–6807.

Gosselin-Grenet, A.S., Marq, J.B., Abrami, L., Garcin, D., Roux, L., 2007. Sendai virus budding in the course of an infection does not require Alix and VPS4A host factors. Virology.

Gotoh, B., Takeuchi, K., Komatsu, T., Yokoo, J., 2003. The STAT2 activation process is a crucial target of Sendai virus C protein for the blockade of alpha interferon signaling. J. Virol. 77 (6), 3360–3370.

Grogan, C.C., Moyer, S.A., 2001. Sendai virus wild-type and mutant C proteins show a direct correlation between L polymerase binding and inhibition of viral RNA synthesis. Virology 288 (1), 96–108.

Horikami, S.M., Hector, R.E., Smallwood, S., Moyer, S.A., 1997. The Sendai virus C protein binds the L polymerase protein to inhibit viral RNA synthesis. Virology 235 (2), 261–270.

Howard, T.L., Stauffer, D.R., Degnin, C.R., Hollenberg, S.M., 2001. CHMP1 functions as a member of a newly defined family of vesicle trafficking proteins. J. Cell Sci. 114 (Pt 13), 2395–2404.

Irie, T., Harty, R.N., 2005. L-domain flanking sequences are important for host interactions and efficient budding of vesicular stomatitis virus recombinants. J. Virol. 79 (20), 12617–12622.

Irie, T., Licata, J.M., Jayakar, H.R., Whitt, M.A., Bell, P., Harty, R.N., 2004a. Functional analysis of late-budding domain activity associated with the PSAP motif within the vesicular stomatitis virus M protein. J. Virol. 78 (14), 7823–7827.

Irie, T., Licata, J.M., McGettigan, J.P., Schnell, M.J., Harty, R.N., 2004b. Budding of PPxY-containing rhabdoviruses is not dependent on host proteins TGS101 and VPS4A. J. Virol. 78 (6), 2657–2665.

Irie, T., Licata, J.M., Harty, R.N., 2005. Functional characterization of Ebola virus L-domains using VSV recombinants. Virology 336 (2), 291–298.

Irie, T., Shimazu, Y., Yoshida, T., Sakaguchi, T., 2007. The YLDL sequence within Sendai virus M protein is critical for budding of virus-like particles and interacts with Alix/AIP1 independently of C protein. J. Virol. 81 (5), 2263–2273.

Jayakar, H.R., Murti, K.G., Whitt, M.A., 2000. Mutations in the PPPY motif of vesicular stomatitis virus matrix protein reduce virus budding by inhibiting a late step in virion release. J. Virol. 74 (21), 9818–9827.

Kato, A., Ohnishi, Y., Kohase, M., Saito, S., Tashiro, M., Nagai, Y., 2001. Y2, the smallest of the Sendai virus C proteins, is fully capable of both counteracting the antiviral action of interferons and inhibiting viral RNA synthesis. J. Virol. 75 (8), 3802–3810.

Katoh, K., Shibata, H., Suzuki, H., Nara, A., Ishidoh, K., Kominami, E., Yoshimori, T., Maki, M., 2003. The ALG-2-interacting protein Alix associates with CHMP4b, a human homologue of yeast Snf7 that is involved in multivesicular body sorting. J. Biol. Chem. 278 (40), 39104–39113.

Katoh, K., Shibata, H., Hatta, K., Maki, M., 2004. CHMP4b is a major binding partner of the ALG-2-interacting protein Alix among the three CHMP4 isoforms. Arch. Biochem. Biophys. 421 (1), 159–165.

Komatsu, T., Takeuchi, K., Yokoo, J., Gotoh, B., 2002. Sendai virus C protein impairs both phosphorylation and dephosphorylation processes of Stat1. FEBS Lett. 511 (1–3), 139–144.

Koyama, A.H., Irie, H., Kato, A., Nagai, Y., Adachi, A., 2003. Virus multiplication and induction of apoptosis by Sendai virus: role of the C proteins. Microbes Infect. 5 (5), 373–378.

Lamb, R.A., Parks, G.D., 2006. Paramyxoviridae: the viruses and their replication, In: Knipe, D.M., Howley, P.M. (Eds.), 5th ed. Fields Virology, vol. 1. Lippincott, Williams & Wilkins, Philadelphia, PA.

Marq, J.B., Brini, A., Kolakofsky, D., Garcin, D., 2007. Targeting of the Sendai virus C protein to the plasma membrane via a peptide-only membrane anchor. J. Virol. 81 (7), 3187–3197.

Matsuo, H., Chevallier, J., Mayran, N., Le Blanc, I., Ferguson, C., Faure, J., Blanc, N.S., Matile, S., Dubochet, J., Sadoul, R., Parton, R.G., Vilbois, F., Gruenberg, J., 2004. Role of LBPA and Alix in multivesicular liposome formation and endosome organization. Science 303 (5657), 531–534.

Mottet, G., Muhlemann, A., Tapparel, C., Hoffmann, F., Roux, L., 1996. A Sendai virus vector leading to the efficient expression of mutant M proteins interfering with virus particle budding. Virology 221 (1), 159–171.

Neumann, G., Ebihara, H., Takada, A., Noda, T., Kobasa, D., Jasenosky, L.D., Watanabe, S., Kim, J.H., Feldmann, H., Kawaoka, Y., 2005. Ebola virus VP40 late domains are not essential for viral replication in cell culture. J. Virol. 79 (16), 10300–10307.

Patton, G.S., Morris, S.A., Chung, W., Bieniasz, P.D., McClure, M.O., 2005. Identification of domains in Gag important for prototypic foamy virus egress. J. Virol. 79 (10), 6392–6399.

Sakaguchi, T., Kato, A., Sugahara, F., Shimazu, Y., Inoue, M., Kiyotani, K., Nagai, Y., Yoshida, T., 2005. AIP1/Alix is a binding partner of Sendai virus C protein and facilitates virus budding. J. Virol. 79 (14), 8933–8941.

Schmitt, A.P., Leser, G.P., Waning, D.L., Lamb, R.A., 2002. Requirements for budding of paramyxovirus simian virus 5 virus-like particles. J. Virol. 76 (8), 3952–3964.

Schmitt, A.P., Leser, G.P., Morita, E., Sundquist, W.I., Lamb, R.A., 2005. Evidence for a new viral late-domain core sequence, FPIV, necessary for budding of a paramyxovirus. J. Virol. 79 (5), 2988–2997.

Slagsvold, T., Pattni, K., Malerod, L., Stenmark, H., 2006. Endosomal and non-endosomal functions of ESCRT proteins. Trends Cell Biol. 16 (6), 317–326.

Strack, B., Calistri, A., Craig, S., Popova, E., Gottlinger, H.G., 2003. AIP1/ALIX is a binding partner for HIV-1 p6 and EIAV p9 functioning in virus budding. Cell 114 (6), 689–699.

Stricker, R., Mottet, G., Roux, L., 1994. The Sendai virus matrix protein appears to be recruited in the cytoplasm by the viral nucleocapsid to function in viral assembly and budding. J. Gen. Virol. 75 (Pt 5), 1031–1042.

Sugahara, F., Uchiyama, T., Watanabe, H., Shimazu, Y., Kuwayama, M., Fujii, Y., Kiyotani, K., Adachi, A., Kohno, N., Yoshida, T., Sakaguchi, T., 2004. Paramyxovirus Sendai virus-like particle formation by expression of multiple viral proteins and acceleration of its release by C protein. Virology 325 (1), 1–10.

Takeuchi, K., Komatsu, T., Yokoo, J., Kato, A., Shioda, T., Nagai, Y., Gotoh, B., 2001. Sendai virus C protein physically associates with Stat1. Genes Cells 6 (6), 545–557.

Thery, C., Boussac, M., Veron, P., Ricciardi-Castagnoli, P., Raposo, G., Garin, J., Amigorena, S., 2001. Proteomic analysis of dendritic cell-derived exosomes: a secreted subcellular compartment distinct from apoptotic vesicles. J. Immunol. 166 (12), 7309–7318.

von Schwedler, U.K., Stuchell, M., Muller, B., Ward, D.M., Chung, H.Y., Morita, E., Wang, H.E., Davis, T., He, G.P., Cimbora, D.M., Scott, A., Krausslich, H.G., Kaplan, J., Morham, S.G., Sundquist, W.I., 2003. The protein network of HIV budding. Cell 114 (6), 701–713.

Welman, A., Burger, M.M., Hagmann, J., 2000. Structure and function of the C-terminal hypervariable region of K-Ras4B in plasma membrane targetting and transformation. Oncogene 19 (40), 4582–4591.